

1 **Evolution of the oligotrophic West Pacific Warm Pool during the Pliocene**

2 Himanshu Bali<sup>1</sup>, Anil K. Gupta<sup>1\*</sup>, Kuppusamy Mohan<sup>2</sup>, K. Thirumalai<sup>3</sup>, Sameer K Tiwari<sup>4</sup>,  
3 Mruganka K. Panigrahi<sup>1</sup>

4 <sup>1</sup> Department of Geology and Geophysics, Indian Institute of Technology, Kharagpur  
5 721302, India

6 <sup>2</sup> School of Mechanical and Building Sciences, VIT University Chennai Campus, Chennai,  
7 600127, India

8 <sup>3</sup> Department of Geosciences, University of Arizona, Tucson, AZ 85721

9 <sup>4</sup> Wadia Institute of Himalayan Geology, Dehradun 248001, India.

10 \*Corresponding author: [anilg@gg.iitkgp.ac.in](mailto:anilg@gg.iitkgp.ac.in)

11 **Key Points:**

- 12 • Evolution of the western Pacific surface paleoceanography during the Pliocene
- 13 • Linkages between evolution of West Pacific Warm Pool and shrinking of Indonesian
- 14 seaway
- 15 • The oligotrophic West Pacific Warm Pool began to develop at ~3.15 Ma

16

17 **Abstract**

18 This study investigates the timing of development of the oligotrophic conditions and  
19 thickening of the West Pacific Warm Pool (WPWP) during the Pliocene. It has been  
20 hypothesized that the evolution of the WPWP and the establishment of equatorial Pacific  
21 zonal gradients are closely related to the narrowing of the Indonesian seaway (IS) as well as  
22 the closure of the Panama gateway; however, the timing of these events remain debated. Here  
23 we analysed planktic foraminiferal abundances combined with stable oxygen and carbon  
24 isotope ratios since the Pliocene at ODP Hole 807A, western Pacific and DSDP Site 214,  
25 eastern Indian Ocean. A comparison of the population of mixed-layer species (MLS) from  
26 both study sites shows a significant increase between ~3.15 and 1.6 Ma. On the contrary,  
27 *Globigerinita glutinata* shows a decrease in its population during this time, indicating  
28 oligotrophic conditions in the western tropical Pacific. The  $\delta^{13}\text{C}$  ratio of epibenthic  
29 foraminiferal species shows a decreasing trend from ~3.15 to ~2.0 Ma, indicating the  
30 lowering of productivity during this interval. Our data suggest that the WPWP developed  
31 around ~3.15 Ma and was closely linked to the gradual closure of the IS.

32 **Keywords:** West Pacific Warm Pool, planktic foraminifera, Pliocene, Mixed-layer species,  
33 oxygen and carbon isotopes, Indonesian seaway.

34 **1. Introduction**

35 The West Pacific Warm Pool (WPWP) encompasses most of the tropical–subtropical  
36 area ( $>30 \times 10^6 \text{ km}^2$ ) of the western Pacific (Cane and Molnar, 2001) and is characterized by  
37 warm surface waters with an annual sea-surface temperature (SST) of  $>28^\circ\text{C}$  (Yan et al.,  
38 1992; Webster and Palmer, 1997) (Fig. 1). The WPWP is  $\sim 2\text{--}5^\circ\text{C}$  warmer than any other  
39 equatorial region and stores large amount of heat (Yan et al., 1992). Thus any change in the

40 size and temperature of the WPWP affects global heat transport from the equator to poles and  
41 also play a role in the evolution of El-Niño-Southern Oscillation (ENSO) events (Meyers et  
42 al., 1996; Sun, 2003; de Garidel-Thoron et al., 2005). Easterly trade winds keep the WPWP  
43 towards the western equatorial Pacific (WEP) under normal conditions (Li et al., 2006),  
44 although its position fluctuates during ENSO events. Oceanographically, the WPWP is  
45 composed of a thick and warm mixed-layer with a consequently deep thermocline (~200 m)  
46 that contrasts with the eastern equatorial Pacific (EEP), which contains a shallow thermocline  
47 and smaller mixed-layer (Fig. 2). This tilt in the thermocline makes the eastern Pacific more  
48 productive than the West (Ravelo et al., 2006). About 10–15 Sv ( $1 \text{ Sv}=10^6 \text{ m}^3\text{s}^{-1}$ ) of low-  
49 salinity, warm water enters the eastern Indian ocean from the WPWP annually (Chong et al.,  
50 2000; Ganachaud and Wunsch, 2000) and is termed the Indonesian Throughflow (ITF). The  
51 ITF transports heat from the WEP north of the equator to 12°S into the eastern Indian Ocean,  
52 mostly through the Makassar Strait (Gordon et al., 1999), and varies on annual, interannual,  
53 and (multi-)decadal timescales (Linsley et al., 2010). Variability in the ITF thus influences  
54 global climates on both short (El-Niño-Southern Oscillation or ENSO-related) and long-term  
55 or tectonic timescales (Schott and McCreary, 2001). Observations indicate that fluctuations in  
56 ENSO and related changes in the Indian monsoon system are linked to major influxes of  
57 Pacific freshwater and heat into the Indian Ocean (Vranes et al., 2002), wherein ITF transport  
58 is greater during La-Niña events compared to El-Niño events. (Gordon and Fine, 1996).

## 59 **2. Evolution of the West Pacific Warm Pool (WPWP)**

60 Small changes related to the dimensions of the oceanic seaways can influence ocean  
61 circulation and heat distribution, and may therefore have a profound impact on the global  
62 climate and ocean productivity (Cane and Molnar, 2001; Nathan and Leckie, 2009).  
63 Progressive narrowing of the Indonesian seaway (IS) is purported to have played a key role in

64 altering and redirecting ocean currents and causing climate change in the tropical eastern  
65 Indian and western Pacific Oceans. Numerous investigations have hypothesized that the  
66 constriction and closure of the IS, the closure of the Panama gateway, and the development of  
67 the WPWP are closely linked (Keller, 1985; Kennett et al., 1985; Chaisson and Ravelo, 2000;  
68 Jian et al., 2006; Li et al., 2006; Nathan et al., 2009). Kennett et al. (1985) and Keller (1985)  
69 used planktic foraminiferal faunal abundance and isotopes to investigate surface and  
70 subsurface circulation changes in the equatorial Pacific, including the Equatorial Under  
71 Current (EUC) over the Miocene. These studies found a gradual shoaling of the EUC towards  
72 the EEP over the past 10 Myr, and concluded that this was due to the narrowing of the IS and  
73 subsequent closure of the Panama gateway. Chaisson and Ravelo (2000) used planktic  
74 foraminiferal data from the WEP and EEP to suggest that the east–west thermocline tilt  
75 developed in the equatorial Pacific during 4.5 to 4 Ma and was related to the closure of the  
76 Panama gateway. Contrastingly, Jian et al. (2006) posited a much earlier formation of the  
77 WPWP using planktic foraminiferal records in the South China Sea and related it to the  
78 closure of the IS during 11.5 to 10.6 Ma.

79  
80 Studies of climate simulations also provide disparate answers regarding the timing of  
81 the development of the WPWP. Model results from Cane and Molnar, (2001) have suggested  
82 that the northward movement of New Guinea during the Pliocene, which effectively prevents  
83 the transport of warm, saline South Pacific waters into the Indian Ocean, is key to the  
84 establishment of the WPWP. On the other hand, Nathan et al. (2009) have shown that  
85 decreasing sea-level around 11-10 Ma led to the development and intensification of the  
86 WPWP. Results based on multi-species foraminiferal isotopic analyses and assemblages of  
87 equatorial Pacific deep-sea cores suggest the evolution of the modern WPWP after ~3.6–3.0  
88 Ma in the Pliocene (Chaisson, 1995; Cannariato and Ravelo, 1997; Chaisson and Ravelo,

89 2000; Ravelo et al., 2006; Sato et al., 2008). Therefore, despite significant progress in the  
90 understanding of closure of the IS and evolution of the WPWP, the timing of the tectonic  
91 constriction of the IS still remains debatable with estimates of age ranging from ~17 to 3 Ma  
92 (Kennett et al., 1985; Jian et al., 2006; Li et al., 2006).

93 Here we produce a 5 Myr record of planktic foraminiferal abundances and a record of  
94 stable isotope composition ( $\delta^{13}\text{C}$ ) of epibenthic foraminifera from Ocean Drilling Program  
95 (ODP) Hole 807A and DSDP Site 214 to constrain the evolution of the WPWP. We compare  
96 our results with those from the WEP (ODP Site 806), EEP (ODP Sites 846 and 850), South  
97 China Sea (SCS) (ODP Sites 1143, 1147/1148) and a site offshore eastern New Zealand  
98 (ODP Site 1125, north slope of Chatham Rise) to explore the spatiotemporal variability of  
99 regional paleoceanography. Finally, we discuss the implications of our dataset and analyses  
100 to the timing of the IS and the evolution of the WPWP.

### 101 **3. Materials and Methods**

102 Five hundred eleven core samples were procured from Ocean Drilling Program  
103 (ODP) Hole 807A, Leg 130, western Pacific under sample request No. #16790A by AKG for  
104 the proposed study. Standard procedures were followed in sample preparation (Gupta and  
105 Thomas, 1999, 2003) with necessary precautions to avoid contamination. The sample  
106 processing was carried out in the Sample Processing Unit of the Paleoceanography and  
107 Paleoclimatology Laboratory, Department of Geology and Geophysics, IIT Kharagpur. The  
108 sliced samples were kept in zip lock bags and carefully labelled. 63 $\mu\text{m}$  size sieve and a jet of  
109 water was used to wash the samples. Contamination was avoided by staining the sieve with  
110 methylene blue solution after each wash so that residual microfossils were stained and easily  
111 identified. Washed samples were transferred to beakers, and oven dried at ~50° C

112 temperatures. The dried samples were then transferred into glass vials labelled with sample  
113 numbers.

### 114 **3.1 Age Model**

115 The age model used in this study is adopted from the Scientific Reports of ODP Leg  
116 130 (Berggren et al. 1995a, 1995b) based on nannofossil and foraminiferal datums. Age  
117 control points are presented in Table 1 and have been updated following the recent geological  
118 timescale (Gradstein et al., 2012) (Fig. 3). The age of each sample was interpolated thereby  
119 yielding a time resolution of ~20 kyr per sample.

### 120 **3.2 Sample Analysis: Census counts**

121 271 samples from ODP Hole 807A, western Pacific, and 267 samples from DSDP  
122 Site 214, eastern Indian Ocean were used to generate planktic data. Processed samples from  
123 ODP Hole 807A were analyzed for mixed-layer species (MLS) of planktic foraminifera. Dry  
124 149  $\mu\text{m}+$  size fraction was split into suitable aliquots to obtain approximately 300 specimens  
125 of planktic foraminifera which were then identified and counted as percentages of overall  
126 species (Schmiedl et al., 1997, 2003; den Dulk et al., 1998; Gupta and Thomas, 2003; Gupta  
127 et al., 2004).

128 To investigate changes in the mixed-layer, we used the census counts of MLS which  
129 included *Globigerinoides extremus*, *Globigerinoides sacculifer*, *Globigerinoides fistulosus*,  
130 *Globigerinoides ruber*, and *Globigerinoides obliquus*. Carbon isotope ( $\delta^{13}\text{C}$ ) analyses were  
131 performed on epibenthic species *Cibicides wuellerstorfi* and *Cibicides kullenbergi* to  
132 understand deep-sea oceanic changes.

133

### 134 **3.3 Stable Isotope ( $\delta^{13}\text{C}$ ) measurements**

135 Benthic foraminiferal tests were used to measure stable carbon isotope ratios from  
136 ODP Hole 807A. 128 samples were analyzed in the Stable Isotope Ratio Mass Spectrometer  
137 (Delta V Plus model from Thermo Fisher) Laboratory, Wadia Institute of Himalayan  
138 Geology, Dehradun, India. Each sample consisted of 8-10 individuals of benthic foraminifera  
139 *Cibicides wuellerstorfi* and *Cibicides kullenbergi* from the >125-micron size fraction.  
140 Methanol and subsequent sonification was used to clean the foraminifera to remove unwanted  
141 clay and other particles that were present within the test. Benthic foraminifer tests amounting  
142 to ~100-300 µg were kept in a sealed glass vial for  $\delta^{13}\text{C}$  analysis and ultra-pure He gas was  
143 introduced to remove the pre-existing gasses. ~99 % orthophosphoric acid was added in the  
144 vial to react with the samples for 60 minutes at 72°C. Headspace sampling of released  $\text{CO}_2$   
145 was achieved by a double-hole needle connected to a PAL auto-sampler followed by the  
146 removal of water by passing it through a Nafion Tube. To remove  $\text{N}_2$ , in order to collect pure  
147  $\text{CO}_2$ , the collected gas was released into a Gas Chromatograph (GC) Column through a  
148 VALCO system. Subsequently, the purified  $\text{CO}_2$  was then introduced in to the Mass  
149 Spectrometer for isotopic measurements.

150 Secondary laboratory standards which were measured against NBS-18 [Value?] were  
151 used for day-to-day measurement and to scale all isotope data to Vienna Peedee Belemnite  
152 (VPDB). These are Merck Carbonate from Merck ( $\delta^{13}\text{C} = -46.95 \pm 0.02 \text{ ‰ VPDB}$ ) and  
153 WIHG-STD-2 ( $\delta^{13}\text{C} = -4.9 \pm 0.01 \text{ ‰ VPDB}$ ) prepared from Mussoorie Limestone. The  
154 secondary standard was used to check long- term reproducibility as well as inter-laboratory  
155 calibration. For the accuracy and consistency of results, a laboratory standard (Merck  $\text{CaCO}_3$   
156 calibrated against NBS-18) was run several times. Repeat tests and measurements of  
157 secondary laboratory standards indicate that the accuracy for carbon and oxygen isotope  
158 measurements is better than ~0.1‰ (1SD).

## 159 **4 Results**

160 Five mixed-layer species of planktic foraminifera were selected to examine  
161 paleoceanographic changes in the mixed-layer at Hole 807A. These species are  
162 *Globigerinoides extremus*, *Globigerinoides sacculifer*, *Globigerinoides fistulosus*, *Globigerinoides*  
163 *ruber* and *Globigerinoides obliquus*. The MLS census data from Hole 807A and Site 214 show  
164 a near similar trend during ~3.15 Ma to 1.6 Ma (Fig. 5c). The MLS data shows a gradual  
165 increase in their population at both sites 807 and 214 beginning at ~3.6 Ma, with an abrupt  
166 increase at ~3.15 Ma. At Hole 807A, the MLS abundances range from 0.3 to a maximum of  
167 31.6% whereas at DSDP Site 214, the MLS population ranges from 1.4 to a maximum of  
168 42.3% with a rapid change occurring at ~2.4 Ma. In contrast to the MLS, *Globigerinita*  
169 *glutinata*, an open-ocean paleoproductivity indicator species [Citation?], shows a drop in its  
170 population starting at ~3.15 Ma and continuously decreasing up to ~1.6 Ma, which suggests  
171 lowered productivity (Fig. 5a). Over this period, between ~3.15 and 2.1 Ma, the  $\delta^{13}\text{C}$  of  
172 benthic foraminifera decreased from 0.02 to 1.2‰, and also indicate low productivity (Fig.  
173 5b). These results suggest the gradual development of a thick mixed-layer (oligotrophic) and  
174 hints at the evolution of the WPWP during the late Pliocene.

## 175 **5 Discussion**

176 Our data from the western Pacific reveals pronounced changes in the surface-ocean  
177 during the Pliocene. The increase in mixed-layer species at Hole 807A suggests the  
178 thickening of the mixed-layer (perhaps accompanied by thermocline deepening) in the  
179 western Pacific beginning at ~3.15 Ma (Fig. 4). The mixed-layer taxa, in general, are  
180 oligotrophic, flourishing in a well-stratified water column and are less abundant in upwelling  
181 systems (Brock et al., 1992). Chaisson and Ravelo (2000) linked the formation of the WPWP  
182 to a dramatic increase in the Walker Circulation and suggested that the piling of warm

183 surface water by the trade winds made a thicker warm pool after the closure of the IS. The  
184 MLS population trend at Hole 807A nearly follows that of DSDP Site 214 between ~3.15 and  
185 1.6 Ma. This suggests that surface-ocean changes at both the sites were near-synchronous and  
186 underpins a linkage between the formation of the WPWP and the closure of the IS.

187 *Globigerinita glutinata* has a wide latitudinal occurrence, and can tolerate a rather  
188 wide range of temperature from 14 to 30°C and 34.4 to 36.4 psu salinities (Bé and Hutson,  
189 1977), and is moderately vulnerable to dissolution. *G. glutinata* is also known to be found in  
190 high abundances in the mid-to-high latitudes as well as in marginal upwelling areas in the  
191 low-latitudes (Fairbanks et al., 1982; Thunell and Reynolds, 1984; Pflaumann and Jian, 1999;  
192 Kawahata et al., 2002). However, the distribution of *G. glutinata* is mainly linked to the  
193 changes in paleoproductivity (Schiebel et al., 2001). According to our dataset, *Globigerinita*  
194 *glutinata* shows an opposite trend as compared to the MLS with a step-wise decrease from  
195 ~3.15 to 1.6 Ma at Hole 807A, indicating deepening of the thermocline and/or increased  
196 oligotrophic conditions (Fig. 4).

197 The WPWP was expanded over most parts of the tropics during the early Pliocene.  
198 The warm pool then gradually contracted toward the equator (Brierley et al., 2009). To  
199 reconstruct the zonal and meridional contraction of the Warm Pool we compared our data  
200 with previous work from the EEP, WEP and SCS. Comparing *G. glutinata* abundances and  
201 MLS data at Hole 807A with the  $\delta^{18}\text{O}$  value differences ( $\Delta\delta^{18}\text{O}$ ) between *N. dutertrei*  
202 (thermocline dweller) and *G. sacculifer* at Site 806, where smaller  $\Delta\delta^{18}\text{O}$  (*G. sacculifer*-*N.*  
203 *dutertrei*) values at Site 806 suggest deepening of the thermocline under a thickening of the  
204 WPWP (Chaisson and Ravelo, 2000), we suggest that thickening of the mixed-layer began at  
205 ~3.15 Ma (Fig. 5a, c).

206 Miller et al. (2012) reported a relatively low sea level between 3.45 and 3.25 Ma.  
207 Consequently the ITF decreased significantly, but the heat flow from the Pacific to the Indian

208 Ocean did not cease completely. However, the Indo-Pacific heat transfer re-established with  
209 the major transgression around 3.25 Ma (De Vleeschouwer, D et al., 2019). Our *G. glutinata*  
210 data shows an increase in its population beginning at ~3.4 Ma. The increase in its population  
211 could be related to the thermocline shoaling in the western Pacific as a result of low sea level.  
212 Our MLS data at both the sites suggest that the onset of the modern oligotrophic WPWP  
213 occurred at ~3.15 Ma. Prior to ~3.15 Ma we do not see any change in the MLS data at either  
214 sites 807 and 214. Weak Walker Circulations (WC) due to the weak zonal SST contrast in the  
215 Pacific could be the reason for the disappearance of the warm pool in the western Pacific  
216 before ~3.15 Ma (CITE Tierney et al. 2019). We suggest that the warm water shifted slowly  
217 in the western Pacific with a gradual reduction in the SST and appearance of Cold Tongue in  
218 the EEP since ~3.15 Ma (Fig 5e). The WC intensified with a gradual increase in the  
219 equatorial Pacific SST contrast between west Pacific and east Pacific. The WC strengthened  
220 and pushed warm water to the western Pacific which eventually piled up in the region leading  
221 to the establishment of the WPWP.

222 Lawrence et al. (2006) have shown an increase in primary productivity in the eastern  
223 Pacific using alkenone concentrations ( $C_{37}$  Total) at Site 846. The primary productivity in the  
224 EEP is closely linked to the intermediate nutrient-rich cold waters from high latitudes of  
225 North and South Pacific. The South Pacific contributes more nutrients to the waters that are  
226 upwelled in the EEP (Toggweiler et al., 1991; Sarmiento et al., 2004). The intermediate  
227 nutrient rich cold waters from the Southern Ocean high latitudes are transported to the EEP  
228 through the EUC (Toggweiler et al., 1991; Bryden & Brady, 1985).

229 Our results point to a dramatic increase in the EEP primary productivity between ~3  
230 and 1.6 Ma (Fig 5d). The intensification of eastern Pacific upwelling cell has been related to  
231 the gradual development of the zonal SST gradients at this time (Steph et al., 2010; Tierney et  
232 al. 2019). Our MLS population abundances at both Sites 807 and 214 are tightly synchronous

**Comment [KT1]:** <https://agupubs.onlinelibrary.wiley.com/doi/epdf/10.1029/2019GL083802> - this study supports our idea of weakened WC!

233 with the primary production in the EEP (Fig 5c). The SST data from Zhang et al. (2014) at  
234 Site 850 and Herbert et al. (2016) at Site 846 from EEP also show a gradual decrease in the  
235 SST at the same time which indicates thermocline shoaling and appearance of the CT in the  
236 EEP at about ~3.15 Ma (Fig 5e). The northward drift of Australia, which restricted the ITF,  
237 could have led to the global oceanic thermocline shoaling at about 3 Ma (Cane and Molnar,  
238 2001).

239 We propose that the zonal migration of equatorial Pacific Warm water from east to  
240 west started with a gradual decrease in SST and with an appearance of CT in the EEP. These  
241 processes eventually strengthened the WC and tectonic forcing gradually constricted the IS  
242 and restricted ITF strength, thereby strengthening the WPWP. Data from the South China Sea  
243 (SCS) show a reduction in SSTs at ~ 3 Ma at ODP Sites 1147 and 1148 (Jia et al., 2008) at  
244 the edge of the warm pool, whereas at ODP Site 1143 the SST remained relatively stable (Li  
245 et al., 2011). Prior to ~3 Ma, the SST was similar at both the sites. Further, data from the SCS  
246 suggests the contraction of the WPWP towards the equator i.e. towards ODP Hole 807A in  
247 the late Pliocene (Fig. 5g). SST  $U_{37}^k$  data from ODP Site 1125 (Fedorov et al., 2015) also  
248 shows a fall in SST at ~3.15 Ma, suggesting narrowing of the expanded warm pool towards  
249 the equator from the southern ocean during this time (Fig. 5f).

## 250 **6. Conclusions**

251 The evolutionary record of the West Pacific Warm Pool (WPWP) was reconstructed  
252 using foraminiferal abundances and their isotopic signatures at ODP Hole 807A and DSDP  
253 Site 214 in the western equatorial Pacific Ocean and eastern Indian Ocean, respectively. We  
254 find a stark decrease in productivity and increase in mixed-layer thickness beginning around  
255 3.15 Ma at the study sites, suggesting that such surface oceanographic changes were linked to  
256 the development of the Indo-Pacific warm pool. Our findings support previously published  
257 work and provide further evidence for the evolution of the Indo-Pacific warm pool during the

258 late Pliocene. We conclude that evolution of the Indo-Pacific warm Pool was closely linked  
259 to progressive narrowing of the Indonesian seaway. Such a tectono-oceanic change may have  
260 had far-reaching impact on the Asia-African climate regime that might have contributed to  
261 the future course of human evolution.

## 262 **Acknowledgements**

263 We would like to thank Ocean Drilling Program for providing samples (No.  
264 #16790A). We are grateful to Wadia Institute of Himalayan Geology for providing the Stable  
265 isotope facility for this study and IIT Kharagpur for laboratory facilities to carry out this  
266 work. AKG thanks the DST, Government of India, New Delhi for Sir J.C. Bose Fellowship  
267 (No. SR/S2/JCB-80/2011). The data has been uploaded on Zonodo.org  
268 (DOI: <https://doi.org/10.5281/zenodo.3631160>)

269

## 270 **References**

- 271 Auer, G., De Vleeschouwer, D., Smith, R. A., Bogus, K., Groeneveld, J., Grunert, P., &  
272 Gallagher, S. J. (2019). Timing and pacing of Indonesian Throughflow restriction and  
273 its connection to Late Pliocene climate shifts. *Paleoceanography and*  
274 *Paleoclimatology*, 34(4), 635-657.  
275
- 276 Be', A. W. (1977). An ecological, zoogeographic and taxonomic review of recent planktic  
277 foraminifera. *Oceanic micropaleontology*, 1, 1-100.  
278
- 279 Berggren, W. A., Hilgen, F. J., Langereis, C. G., Kent, D. V., Obradivich, J. D., Raffi, I.,  
280 Raymo, M. E., Shackleton, N. J. (1995a). Late Neogene chronology: New  
281 perspectives in high resolution stratigraphy, *Geological Society of American Bulletin*,  
282 Vol. 107, pp. 1272-1287.  
283
- 284 Berggren, W. A., Kent, D. V., Swisher, C. C. III, Aubry, M.-P. (1995b). A revised Cenozoic  
285 geochronology and chronostratigraphy, by Berggren, W. A. (Ed.) *Geochronology,*  
286 *Time scale and Global Stratigraphic Correlation*, The Society of Economic  
287 Paleontologists and Mineralogists Special Publication, Vol. 54, pp. 129- 212.  
288
- 289 Brierley, C. M., Fedorov, A. V., Liu, Z., Herbert, T. D., Lawrence, K. T., & LaRiviere, J. P.  
290 (2009). Greatly expanded tropical warm pool and weakened Hadley circulation in  
291 the early Pliocene. *Science*, 323(5922), 1714-1718.  
292
- 293 Bryden, H. L., & Brady, E. C. (1985). Diagnostic model of the three-dimensional circulation  
294 in the upper equatorial Pacific Ocean. *Journal of Physical Oceanography*, 15(10),  
295 1255–1273. [https://doi.org/10.1175/1520-0485\(1985\)015<1255:DMOTTD>2.0.CO;2](https://doi.org/10.1175/1520-0485(1985)015<1255:DMOTTD>2.0.CO;2)

296 Brock, J.C., McClain, C.R., Anderson, D.M., Prell, W.L. & Hay, W.W. (1992). Southwest  
297 monsoon circulation and environments of recent planktic foraminifera in the  
298 northwestern Arabian Sea. *Paleoceanography*, 7(6): 799-813.  
299

300 Cane, M. A., & Molnar, P. (2001). Closing of the Indonesian seaway as a precursor to east  
301 African aridification around 3–4 million years ago. *Nature*, 411(6834), 157-162.  
302

303 Cannariato, K. G., & Ravelo, A. C. (1997). Pliocene-Pleistocene evolution of eastern tropical  
304 Pacific surface water circulation and thermocline depth. *Paleoceanography*, 12(6),  
305 805-820  
306

307 Chaisson, W.P. (1995). Planktic foraminiferal assemblages and paleoceanographic change in  
308 the trans-tropical Pacific Ocean: A comparison of west (Leg 130) and east (Leg  
309 138), latest Miocene to Pleistocene. *Proceedings of the Ocean Drilling Program,*  
310 *Scientific Results, 138*, pp. 555-597.  
311

312 Chaisson, W. P., & Ravelo, A. C. (2000). Pliocene development of the east-west  
313 hydrographic gradient in the equatorial Pacific. *Paleoceanography*, 15(5), 497-505.  
314

315 Chong, J. C., J. Sprintall, S. Hautala, W. L. Morawitz, N. A. Bray, and W. Pandoe (2000).  
316 Shallow throughflow variability in the outflow straits of Indonesia, *Geophys. Res.*  
317 *Lett.*, 27, 125–128.  
318

319 De Garidel-Thoron, T., Rosenthal, Y., Bassinot, F., Beaufort, L. (2005). Stable sea surface  
320 temperatures in the western Pacific warm pool over the past 1.75 million years.  
321 *Nature* 433, 294–298.  
322

323 den Dulk, M., Reichert, G. J., Memon, G. M., Roelofs, E. M., Zachariasse, W. J., Van der  
324 Zwaan, G. J. (1998). Benthic foraminiferal response to variation in surface water  
325 productivity and oxygenation in the northern Arabian Sea, *Marine*  
326 *Micropaleontology*, Vol. 35, pp. 43-66.

327 Drenkard, E. J., & Karnauskas, K. B. (2014). Strengthening of the Pacific equatorial  
328 undercurrent in the SODA reanalysis: Mechanisms, ocean dynamics, and  
329 implications. *Journal of Climate*, 27(6), 2405-2416.  
330

331 Fairbanks, R. G., Sverdløve, M., Free, R., Wiebe, P. H., and Be', A. W. H. (1982). Vertical  
332 distribution and isotopic fractionation of living planktic foraminifera from the  
333 Panama Basin. *Nature*, Vol. 298, pp. 841-844.  
334

335 Fedorov, A. V., Burls, N. J., Lawrence, K. T., & Peterson, L. C. (2015). Tightly linked zonal  
336 and meridional sea surface temperature gradients over the past five million years.  
337 *Nature Geoscience*, 8(12), 975.  
338

339 Ganachaud, A., and C. Wunsch (2000), Improved estimates of global ocean circulation, heat  
340 transport and mixing from hydrographic data, *Nature*, 408, 453– 457.  
341

342 Gordon, A. L., & Fine, R. A. (1996). Pathways of water between the Pacific and Indian  
343 oceans in the Indonesian seas. *Nature*, 379(6561), 146.  
344

345 Gordon, A. L., Susanto, R. D., & Field, A. (1999). Throughflow within Makassar Strait.  
346 Geophysical Research Letters, 26(21), 3325-3328.  
347

348 Gradstein, F.M., Ogg, J.G., Schmitz, M.D., and Ogg, G.M., eds (2012) The Geological Time  
349 Scale 2012, Amsterdam, Elsevier, 2 vols., 1144 p.  
350

351 Gupta, A.K. and Thomas, E., (1999). Latest Miocene-Pleistocene productivity and deep-sea  
352 ventilation in the northwestern Indian Ocean (DSDP Site 219). *Paleoceanography*,  
353 14, 62-73.  
354

355 Gupta, A. K., and Thomas, E. (2003). Initiation of Northern Hemisphere Glaciation and  
356 strengthening of the northeast Indian monsoon: Ocean Drilling Program site 758,  
357 eastern equatorial Indian Ocean. *Geology*, Vol. 31, pp. 47-50.  
358

359 Herbert, T. D., Lawrence, K. T., Tzanova, A., Peterson, L. C., Caballero-Gill, R., & Kelly, C.  
360 S. (2016). Late Miocene global cooling and the rise of modern ecosystems. *Nature*  
361 *Geoscience*, 9(11), 843.  
362

363 Jia, G., Chen, F., & Peng, P. A. (2008). Sea surface temperature differences between the  
364 western equatorial Pacific and northern South China Sea since the Pliocene and their  
365 paleoclimatic implications. *Geophysical Research Letters*, 35(18).  
366

367 Jian, Z., Yu, Y., Li, B., Wang, J., Zhang, X., Zhou, Z. (2006). Phased evolution of the south-  
368 north hydrographic gradient in the South China Sea since the middle Miocene.  
369 *Palaeogeography, Palaeoclimatology, Palaeoecology* 230, 251–263.  
370

371 Karnauskas, K. B., & Cohen, A. L. (2012). Equatorial refuge amid tropical warming. *Nature*  
372 *Climate Change*, 2(7), 530.  
373

374 Kawahata, H., Nishimura, A., and Gagan, M. K. (2002). Seasonal change in foraminiferal  
375 production in the western equatorial Pacific warm pool: evidence from sediment trap  
376 experiments. *Deep-Sea Research II*, Vol. 49, pp. 2783-2800.  
377

378 Keller, G. (1985). Depth stratification of planktic foraminifers in the Miocene ocean.  
379 *Geological Society of America Memoirs*, 163, 177-196.  
380

381 Kennett, J. P., G. Keller, and M. S. Srinivasan, (1985). Miocene planktic foraminiferal  
382 biogeography and paleogeographic development of the Indo-Pacific region, in *The*  
383 *Miocene Ocean: Paleoceanography and Biogeography*, edited by J. P. Kennett, pp.  
384 197–236.  
385

386 Lawrence, K. T., Liu, Z., & Herbert, T. D. (2006). Evolution of the eastern tropical Pacific  
387 through Plio-Pleistocene glaciation. *Science*, 312(5770), 79-83.  
388

389 Li, L., Li, Q., Tian, J., Wang, P., Wang, H., & Liu, Z. (2011). A 4-Ma record of thermal  
390 evolution in the tropical western Pacific and its implications on climate change.  
391 *Earth and Planetary Science Letters*, 309(1), 10-20.  
392

393 Li, Q., Li, B., Zhong, G., McGowran, B., Zhou, Z., Wang, J., Wang, P. (2006). Late Miocene  
394 development of the western Pacific warm pool: planktic foraminifer and oxygen

395 isotopic evidence. *Palaeogeography, Palaeoclimatology, Palaeoecology* 237, 465–  
396 482.  
397  
398 Linsley, B. K., Rosenthal, Y., & Oppo, D. W. (2010). Holocene evolution of the Indonesian  
399 throughflow and the western Pacific warm pool. *Nature Geoscience*, 3(8), 578.  
400

401 Meyers, G. (1996). Variations of Indonesian throughflow and El Niño - Southern Oscillation,  
402 *J. Geophys. Res.*, 101(C5), 12255–12263.  
403

404 Miller, K. G., Wright, J. D., Browning, J. V., Kulpecz, A., Kominz, M., Naish, T. R., ... &  
405 Sostdian, S. (2012). High tide of the warm Pliocene: Implications of global sea level  
406 for Antarctic deglaciation. *Geology*, 40(5), 407-410.  
407

408 Nathan, S. A., & Leckie, R. M. (2009). Early history of the Western Pacific Warm Pool  
409 during the middle to late Miocene (~ 13.2–5.8 Ma): Role of sea-level change and  
410 implications for equatorial circulation. *Palaeogeography, Palaeoclimatology,*  
411 *Palaeoecology*, 274(3-4), 140-159.  
412

413 Pflaumann, U., & Jian, Z. (1999). Modern distribution patterns of planktonic foraminifera in  
414 the South China Sea and western Pacific: a new transfer technique to estimate  
415 regional sea-surface temperatures. *Marine Geology*, 156(1-4), 41-83.  
416

417 Ravelo, A. C., Dekens, P. S., & McCarthy, M. (2006). Evidence for El Niño-like conditions  
418 during the Pliocene. *GSA today*, 16(3), 4-11.  
419

420 Ryan, J. P., Ueki, I., Chao, Y., Zhang, H., Polito, P. S., & Chavez, F. P. (2006). Western  
421 Pacific modulation of large phytoplankton blooms in the central and eastern  
422 equatorial Pacific. *Journal of Geophysical Research: Biogeosciences*, 111(G2).  
423

424 Sarmiento, J. L., Gruber, N., Brzezinski, M. A., & Dunne, J. P. (2004). High-latitude controls  
425 of thermocline nutrients and low latitude biological productivity. *Nature*, 427(6969),  
426 56.  
427

428 Sato, K., Oda, M., Chiyonobu, S., Kimoto, K., Domitsu, H., & Ingle, J. C. (2008).  
429 Establishment of the western Pacific warm pool during the Pliocene: Evidence from  
430 planktic foraminifera, oxygen isotopes, and Mg/Ca ratios. *Palaeogeography,*  
431 *Palaeoclimatology, Palaeoecology*, 265(1), 140-147.  
432

433 Schiebel, R., Waniek, J., Bork, M., and Hemleben, C. (2001). Planktic foraminiferal  
434 production stimulated by chlorophyll redistribution and entrainment of nutrients.  
435 *Deep Sea Research Part I: Oceanographic Research Papers*, 48(3), 721-740.  
436

437 Schlitzer, R., Ocean Data View, <http://odv.awi.de>, 2014.  
438

439 Schmiedl, G., Mackensen, A. and Muller, P.J. (1997). Recent benthic foraminifera from the  
440 eastern South Atlantic Ocean: Dependence on food supply and water masses. *Marine*  
441 *Micropaleontology*, 32, pp. 249-287.  
442

- 443 Schmiedl, G., Mitschele, A., Beck, S., Emeis, K. -C., Hemleben, C., Schulz, H., Sperling, M.,  
444 Weldeab, S. (2003). Benthic foraminiferal record of ecosystem variability in the  
445 eastern Mediterranean Sea during the times of sapropel S5 and S6, *Palaeogeography,*  
446 *Palaeoclimatology, Palaeoecology*, Vol. 190, pp. 139-164.
- 447
- 448 Schott, F. A, and J. P. McCreary, (2001). The monsoon circulation of the Indian Ocean,  
449 *Progress Oceanogr.*, 51, 1–123.
- 450
- 451 Steph, S., Tiedemann, R., Prange, M., Groeneveld, J., Schulz, M., Timmermann, A., ... &  
452 Haug, G. H. (2010). Early Pliocene increase in thermohaline overturning: A  
453 precondition for the development of the modern equatorial Pacific cold tongue.  
454 *Paleoceanography*, 25(2).
- 455
- 456 Sun, D. Z. (2003), Possible effect of an increase in the warm-pool SST on the magnitude of  
457 El Niño warming, *J. Clim.*, 16, 185–205.
- 458
- 459 Thunell, R. C., & Reynolds, L. A. (1984). Sedimentation of planktic foraminifera: seasonal  
460 changes in species flux in the Panama Basin. *Micropaleontology*, 243-262.
- 461
- 462 Toggweiler, J. R., Dixon, K., & Broecker, W. S. (1991). The Peru upwelling and the  
463 ventilation of the South Pacific thermocline. *Journal of Geophysical Research:*  
464 *Oceans*, 96(C11), 20467-20497.
- 465
- 466 Vranes, K., Gordon, A. L., & Field, A. (2002). The heat transport of the Indonesian  
467 Throughflow and implications for the Indian Ocean heat budget. *Deep Sea Research*  
468 *Part II: Topical Studies in Oceanography*, 49(7-8), 1391-1410.
- 469
- 470 Webster, P.J., Palmer, T.N. (1997). The past and future of El Niño. *Nature* 390, 562–564.
- 471
- 472 Wyrtki, K., & Kilonsky, B. (1984). Mean water and current structure during the Hawaii-to-  
473 Tahiti shuttle experiment. *Journal of Physical Oceanography*, 14(2), 242-254.
- 474
- 475 Yan, X. H., Ho, C. R., Zheng, Q., & Klemas, V. (1992). Temperature and size variabilities of  
476 the Western Pacific Warm Pool. *Science*, 258(5088), 1643-1646.
- 477
- 478 Zhang, Y. G., Pagani, M., & Liu, Z. (2014). A 12-million-year temperature history of the  
479 tropical Pacific Ocean. *Science*, 344(6179), 84-87.
- 480

481

482 **Figure captions:**

483 **Figure 1:** Location of ODP Hole 807A and DSDP Site 214. Background was created using

484 Ocean-Data-View (Schlitzer, 2014). NEC = North Equatorial Current; NECC = North

485 Equatorial Countercurrent; SEC = South Equatorial Current, SECC = South Equatorial

486 Countercurrent; EUC = Equatorial Undercurrent; MC = Mindanao Current; ME = Mindanao  
487 Eddy; HE = Halmahera Eddy.

488 **Figure 2:** Average ocean surface temperature along the equator in the Pacific. Background  
489 was created using Ocean-Data-View (Schlitzer, 2014).

490 **Figure 3:** Depth vs Age plot at ODP Hole 807A based on foraminiferal and nannofossil  
491 datums (Gradstein et al., 2012).

492 **Figure 4:** Percent distribution of *Globorotalia glutinata* (a) and mixed-layer species (b) at  
493 ODP Hole 807A.

494 **Figure 5:** Proxy records at ODP Hole 807A compared with those from the other sites. (a)  
495 Percentage distribution of *Globigerinita glutinata* (present study) and The  $\delta^{18}\text{O}$  differences  
496 ( $\Delta\delta^{18}\text{O}$  values) between *Globigerinoides sacculifer* (surface) and *Neogloboquadrina dutertrei*  
497 (thermocline) dwellers at ODP Site 806 (Chaisson and Ravelo, 2000) (red), (b)  $\delta^{13}\text{C}$  values of  
498 *Cibicides wuellerstorfi* and *Cibicides kullenbergi* at ODP Hole 807A present study), (c) %  
499 Mixed-layer species at ODP Hole 807A and DSDP Site 214 (present study), (d)  
500 Concentration of alkenones  $\text{C}_{37}$  Total (nmol/g) at ODP Site 846 (Lawrence et al., 2006). (e)  
501 SST based on  $\text{U}^{\text{k}}_{37}$  at ODP Site 138-846  $\text{U}^{\text{k}}_{37}$  (Herbert, TD et al., 2016) (green) and SST  
502 based on  $\text{TEX}_{86}$  at ODP 850 (Zhang et al., 2014) (red), (f) SST based on  $\text{U}^{\text{k}}_{37}$  at ODP Site  
503 1125 (Fedorov et al., 2015), (g) SST based on  $\text{U}^{\text{k}}_{37}$  at ODP Site 1143 (Li et al., 2011) and at  
504 ODP Site 1147/1148 (Jia et al., 2008). IG = Indonesian Gateway; WPWP = West Pacific  
505 Warm Pool; MPWP = Mid-Pliocene Warm Period.

506  
507 **Table 1:** The calcareous nannofossil and foraminiferal datums from ODP Hole 807A with  
508 their ages from Berggren et al. (1995a, 1995b) and updated to Gradstein et al. (2012).

509

Datum	Events	Depth	GTS 2012
LAD	<i>P.lacunosa</i> (N)	12.15	0.44
LAD	<i>C.macintyreii</i> (N)	21.65	1.6
LAD	<i>G.fistulosus</i> (F)	31.15	1.88

FAD	<i>G.truncatulinoides (F)</i>	31.15	1.93
LAD	<i>D.tamalis (N)</i>	40.65	2.8
LAD	<i>G.altispira (F)</i>	59.65	3.13
FAD	<i>G.fistulosus (F)</i>	69.15	3.33
LAD	<i>C.acutus (N)</i>	88.15	5.04

510

511

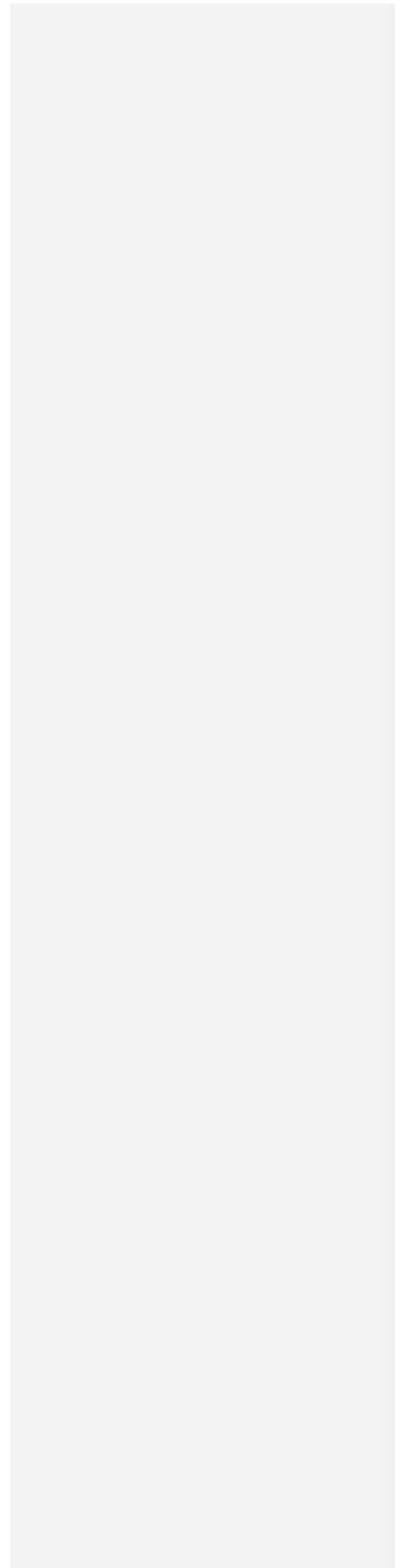


Figure 1.

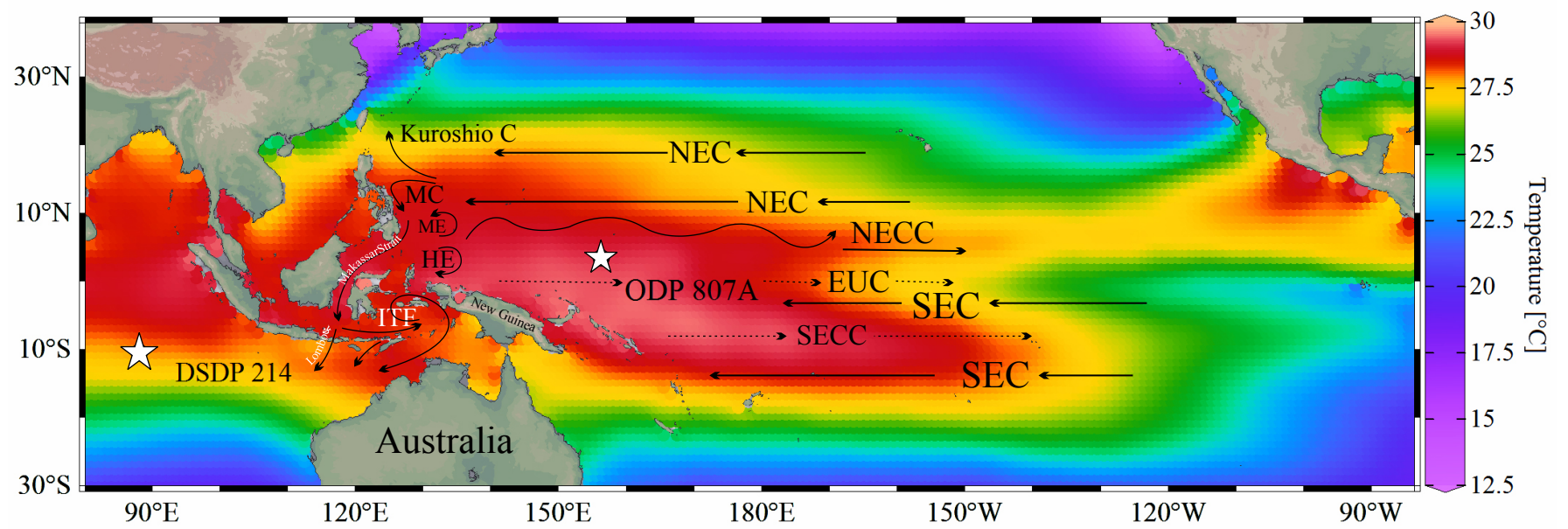


Figure 1: Location of ODP Hole 807A and DSDP Site 214. Background was created using Ocean-Data-View (Schlitzer, 2014). NEC = North Equatorial Current; NECC = North Equatorial Countercurrent; SEC = South Equatorial Current, SECC = South Equatorial Countercurrent; EUC = Equatorial Undercurrent; MC = Mindanao Current; ME = Mindanao Eddy; HE = Halmahera Eddy.

Figure 2.

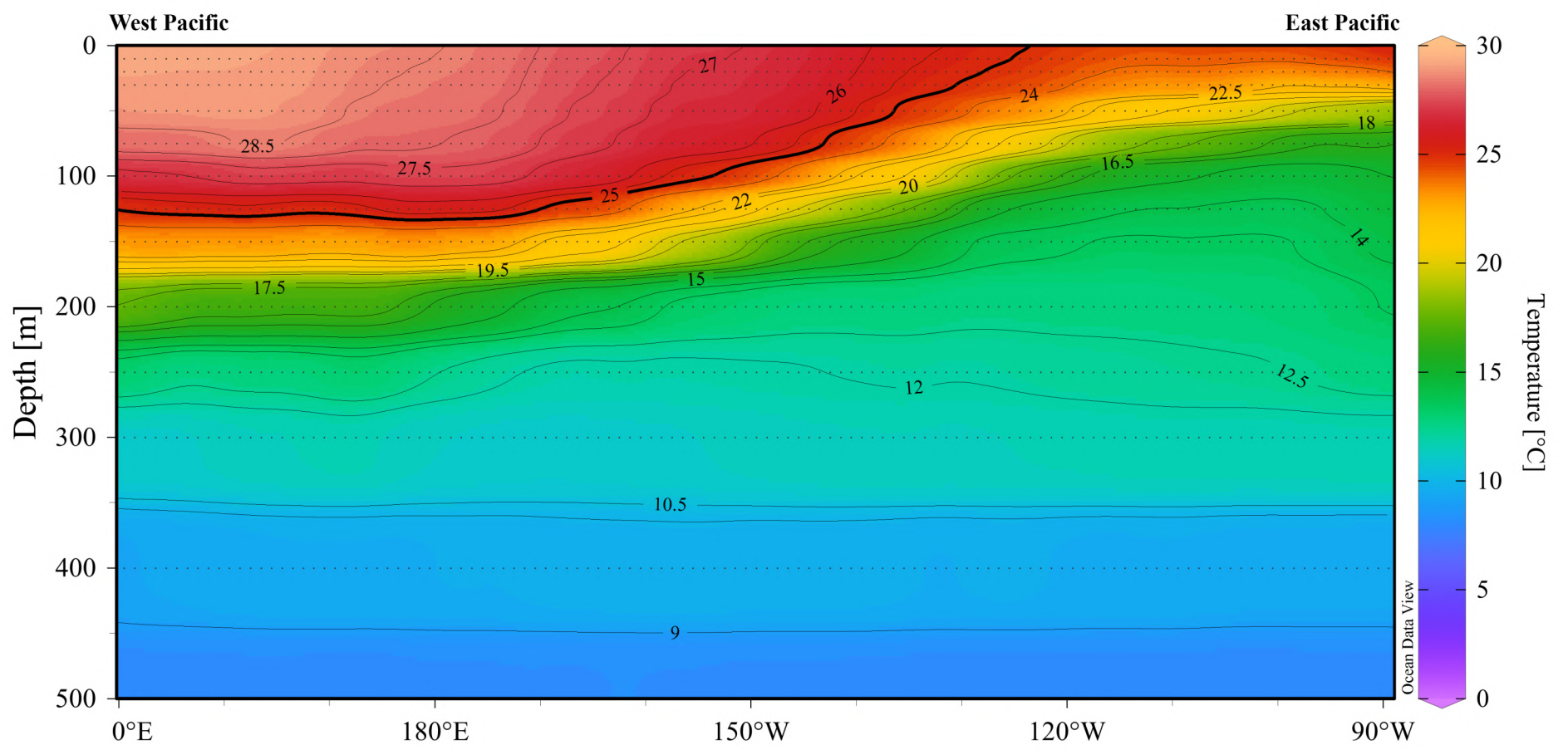


Figure 2: Average ocean surface temperature along the equator in the Pacific.  
Background was created using Ocean-Data-View (Schlitzer, 2014).

Figure 3.

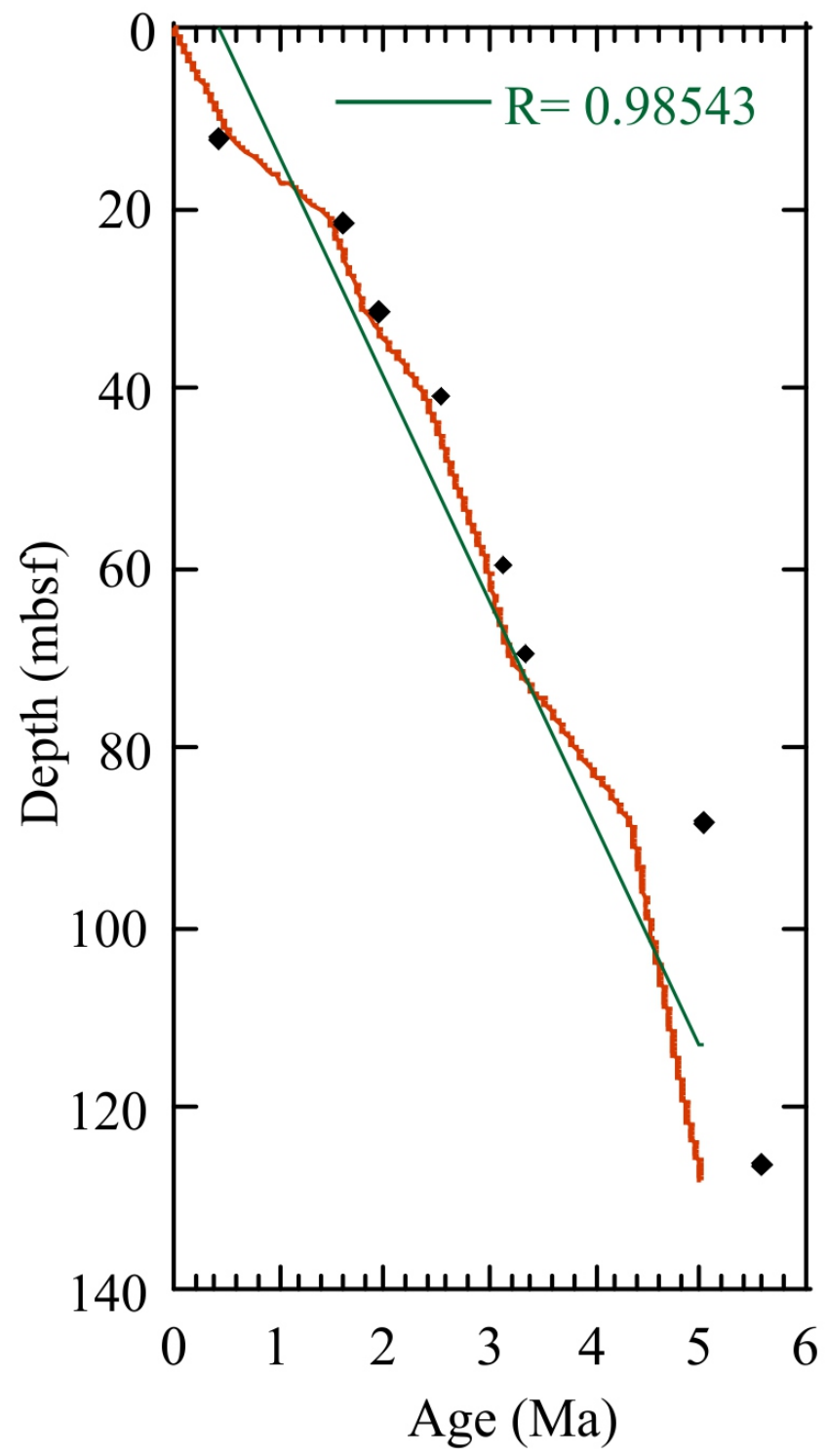


Figure 3: Depth vs Age plot at ODP Hole 807A based on foraminiferal and nannofossil datums (Gradstein et al., 2012).

**Figure 4.**

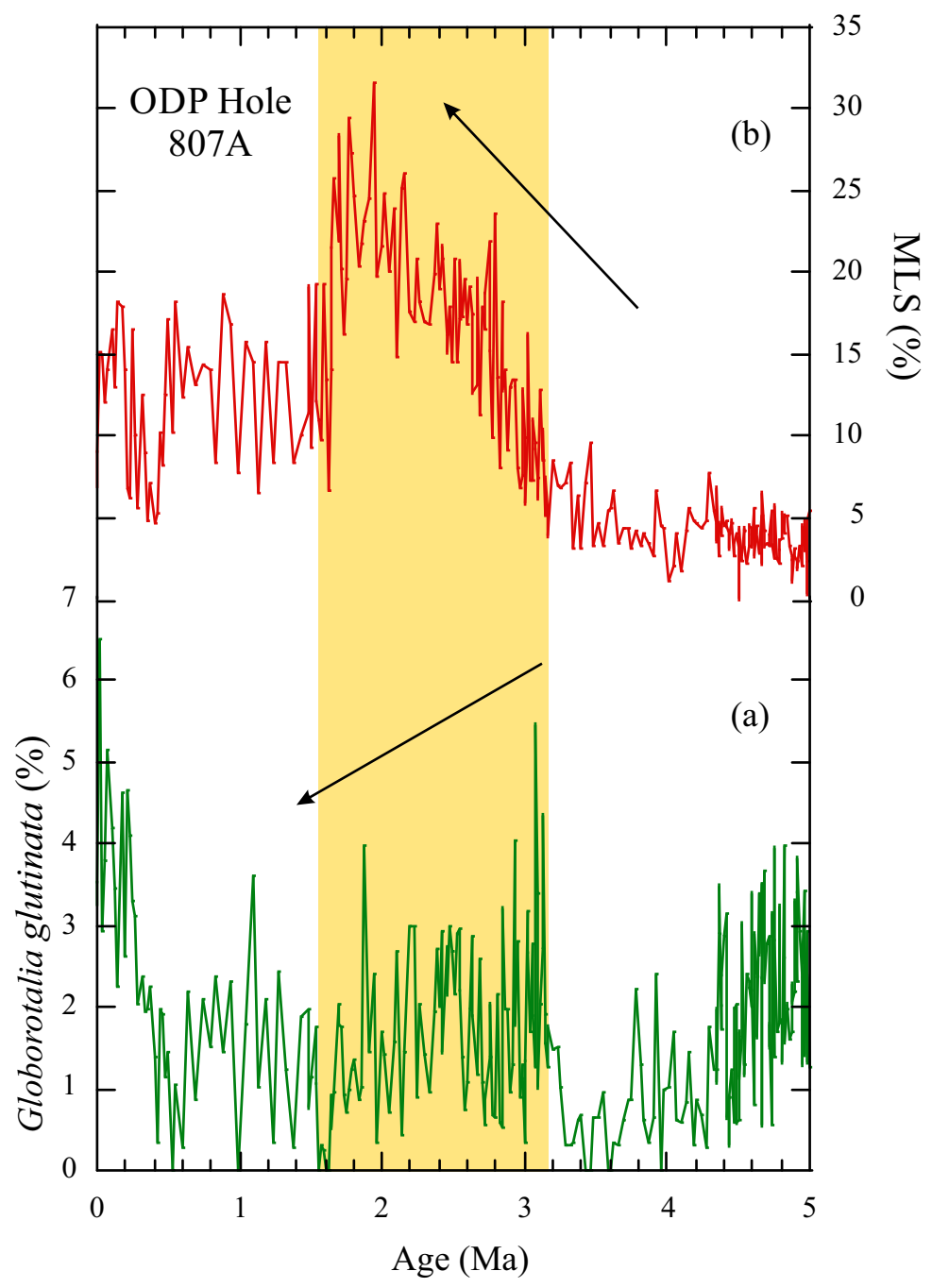


Figure 4: Percentage distribution of *Globorotalia glutinata* (a), % Mixed layer Species (b) at ODP Hole 807A.

Figure 5.

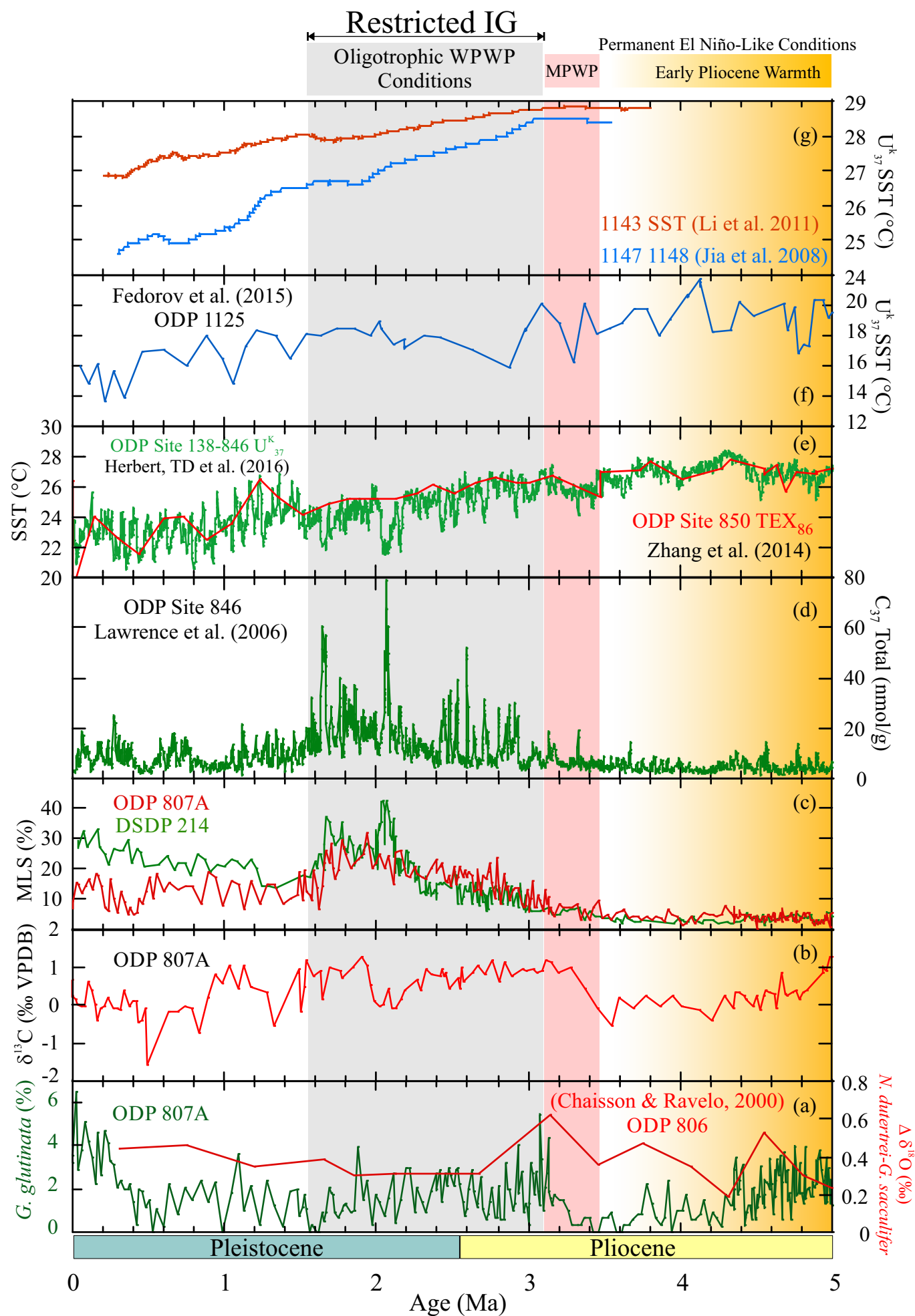


Figure 5: Proxy records at ODP Hole 807A compared with those from the other sites. (a) Percentage distribution of *Globigerinita glutinata* (present study) and The  $\delta^{18}\text{O}$  differences ( $\Delta\delta^{18}\text{O}$  values) between *Globigerinoides sacculifer* (surface) and *Neogloboquadrina dutertrei* (thermocline) dwellers at ODP Site 806 (Chaisson and Ravelo, 2000) (red), (b)  $\delta^{13}\text{C}$  values of *Cibicides wuellerstorfi* and *Cibicides kullenbergi* at ODP Hole 807A present study), (c) % Mixed-layer species at ODP Hole 807A and DSDP Site 214 (present study), (d) Concentration of alkenones  $\text{C}_{37}$  Total (nmol/g) at ODP Site 846 (Lawrence et al., 2006). (e) SST based on  $\text{U}_{37}^{\text{k}}$  at ODP Site 138-846  $\text{U}_{37}^{\text{k}}$  (Herbert, TD et al., 2016) (green) and SST based on  $\text{TEX}_{86}$  at ODP 850 (Zhang et al., 2014) (red), (f) SST based on  $\text{U}_{37}^{\text{k}}$  at ODP Site 1125 (Fedorov et al., 2015), (g) SST based on  $\text{U}_{37}^{\text{k}}$  at ODP Site 1143 (Li et al., 2011) and at ODP Site 1147/1148 (Jia et al., 2008). IG = Indonesian Gateway; WPWP = West Pacific Warm Pool; MPWP = Mid-Pliocene Warm Period.